A crossed beam and ab initio study of the $C_2(X^1\Sigma_g^+ /a^3\prod_u)+ C_2H_2(X^1\Sigma_g^+)$ reactions

Ralf I. Kaiser [a,*], Nadia Balucani [b], Dmitry O. Charkin [c], Alexander M. Mebel [d,1]

[a] *Department of Chemistry, University of Hawai'i at Manoa, 2545 The Mall, Honolulu, HI 96822, USA*
[b] *Dipartimento di Chimica, Università di Perugia, 06123 Perugia, Italy*
[c] *Department of Material Sciences, Lomonosov's Moscow State University, Moscow, Russia*
[d] *Institute of Atomic and Molecular Sciences, 1, Section 4, Roosevelt Road, 107 Taipei, Taiwan, ROC*

Abstract

The reaction dynamics of C_2 in the ground ($^1\Sigma_g^+$) and first electronically excited ($^3\prod_u$) states with the simplest alkyne, acetylene $C_2H_2(X^1\Sigma_g^+)$, were investigated in a crossed molecular beam setup at a nominal collision energy of 24.1 kJ mol^{-1}. The experimental data expose the existence of a C_2/H exchange pathway to form $C_4H + H$. The experimental results were combined with electronic structure calculations on the singlet and triplet C_4H_2 surfaces. The reaction of $C_2(X^1\Sigma_g^+)$ was found to proceed via indirect scattering dynamics through addition of C_2 to the carbon–carbon triple bond. On the triplet surface, $C_2(a^3\prod_u)$ adds also to the acetylenic triple bond. Dominated by large impact parameters, this process favors the formation of two short lived chain-like triplet C_4H_2 isomers. For both reactions, the identification of the butadiynyl radical as a relevant product presents an important step to refine the networks of reactions for the modeling of polycyclic aromatic hydrocarbons formation together with that of their hydrogen deficient precursors in the interstellar medium, in carbon-rich circumstellar envelopes and pre-planetary nebula, and in combustion flames.
© 2003 Elsevier B.V. All rights reserved.

1. Introduction

Gas phase reactions of the dicarbon molecule, C_2, are believed to be relevant in a variety of environments, where such a species has been detected, e.g., in hydrocarbon flames or chemical vapor deposition of diamond [1,2]. Of great interest is certainly the potential role of gas phase C_2 reactions in some celestial bodies, such as the comets where the spectral lines of C_2 in its $^1\Sigma_g^+$ electronic ground state were detected more than a century ago [3–5] and in the interstellar medium. $C_2(X^1\Sigma_g^+)$ transitions were, in fact, observed towards warm carbon stars like IRC + 10216 [6] and post asymptotic giant branch (AGB) stars such as HD 56126 [7]. Due to their importance, the kinetics of reactions involving the ground state and also the electronically excited a $^3\prod_u$ state (lying only 718.32 cm^{-1} above the ground state) have been widely

---
* Corresponding author.
E-mail address: kaiser@gold.chem.hawaii.edu (R.I. Kaiser).
[1] Present address: Department of Chemistry and Biochemistry, Florida National University, Miami, FL 33199, USA.

investigated by following the $C_2(X^1\Sigma_g^+, a^3\prod_u)$ disappearance in the presence of various collision partners. Interestingly, the reactions of $C_2(X^1\Sigma_g^+)$ were found to be of the gas kinetic order when the molecular partner is an unsaturated hydrocarbon, while the $C_2(a^3\prod_u)$ reactions were suggested to be systematically slower [8].

Despite this extensive kinetic investigation, information on the reaction products and involved intermediates is still lacking. In some cases, primary products and reaction mechanisms were speculated on the basis of the observed temperature dependence of the reactions. However, only experiments performed under single collision conditions can elucidate the reaction mechanism at the microscopic level and identify the primary products without the occurrence of collisional stabilization of the involved complexes or successive reaction of the nascent reaction products. The veracity of this statement has been demonstrated with the case of the dicarbon reaction with ethylene, for which a molecular beam study combined with electronic structure calculations of the relevant potential energy surface has revealed that at least the formation of the n-C_4H_3 (and isomers) plus atomic hydrogen is an important reaction pathway [9,10]. Interestingly, this channel was never considered before, while the previously alleged main reaction products, $C_2H + C_2H_3$ ($\Delta_r H = -75.5$ kJ mol^{-1}) or $C_2H_2 + C_2H_2$ ($\Delta_r H = 435.8$ kJ mol^{-1}), were not found to be easily accessible by the system [11].

In this Letter, we expand our studies of dicarbon systems and investigate the reaction of $C_2(X^1\Sigma_g^+, a^3\prod_u)$ with acetylene in a molecular beams setup. We recall that, because of the simultaneous presence of dicarbon and acetylene in many combustion processes and extraterrestial environments, the study of their reaction at a detailed microscopic level is expected to greatly help in the chemical modeling of those complex systems.

2. Experimental

The crossed beam experiment was conducted at a collision energy, E_c, of 24.1 kJ mol^{-1} by using a universal crossed molecular beam apparatus

[12,13]. Briefly, the dicarbon beam of $C_2(X^1\Sigma_g^+/a^3\prod_u)$ was prepared via laser ablation of graphite and seeding the ablated species in helium carrier gas [14]. After the beam passed a skimmer, the chopper wheel, which was located after the ablation zone, selected a slice of the pulsed beam with a peak velocity, v_p, of 1800 ± 10 ms^{-1} and a speed ratio, S, of 6.3 ± 0.2. At this collision energy, the beam contained both ground state and electronically excited dicarbon [9,10] The pulsed dicarbon beam crossed the acetylene beam ($v_p = 900 \pm 5$ ms^{-1}; $S = 12.1 \pm 0.3$) at 90° in the interaction region of the scattering chamber held at about $1 \times 10 E^{-7}$ mbar during the experiment. The reaction products were detected via a rotating quadrupole mass spectrometer, preceded by an electron impact ionizer; the whole detector unit was placed in a rotatable ultra-high-vacuum chamber at pressures of 8×10^{-13} mbar. By employing the time-of-flight (TOF) technique, the product velocity distribution of the reaction product was measured at different laboratory scattering angles and for distinct mass-to-charge ratios (m/e). To extract information on the chemical dynamics, a transformation of coordinates from the laboratory system to the center-of-mass (CM) reference frame is employed [12,13]. This was achieved by forward-convoluting trial CM functions – the product angular, $T(\theta)$, and translational energy, $P(E_T)$, flux distributions – until the best-fit of the laboratory data was obtained.

3. The computational approach

The reactants, products, various intermediates, and transitions states on the potential energy surfaces for the $C_2(^1\Sigma_g^+)/C_2(^3\Pi_u) + C_2H_2$ reactions have been optimized using the hybrid density functional B3LYP method [15,16] with the 6-311G(d,p) basis set. Vibrational frequencies have been also calculated at the B3LYP/6-311G(d,p) level for characterization of stationary points (number of maginary frequencies NIMAG = 0 and 1 for local minima and transition states, respectively) and to obtain zero-point energy (ZPE) corrections. The energies were then refined by single-point coupled cluster [17] CCSD(T)/6-311 + G(3df,2p)

calculations, so that the overall theoretical level can be written as CCSD(T)/6-311 + G(3df,2p)//B3LYP/ 6-311G(d,p) + ZPE[B3LYP/6-311G(d,p)]. All calculations were carried out using the GAUSSIAN 98 [18] and MOLPRO 2000 [19] programs.

4. Results

Reactive scattering signal is observed at mass-to-charge ratio, m/e, of 49 (C_4H^+) and 48 (C_4^+). Since the TOF spectra recorded at both mass-to-charge ratios are superimposable, we conclude that under our experimental conditions the only product in this range of masses has the molecular formula C_4H; the C_4^+ ion actually originates from dissociative ionization of the parent molecule in the ionizer. Note that the ablation beam contains also tricarbon molecules $C_3(X^1\Sigma_g^+)$ [15] which could react in principle with acetylene to form l-C_5H ($X^2\prod_\Omega$) + H($^2S_{1/2}$), $C_5(X^1\Sigma_g^+)$ + $H_2(X^1\Sigma_g^+)$, $C_4H_2(X^1\Sigma_g^+)$ + C (^3P_j), and $C_4H(X^2\Sigma^+)$ + CH ($X^2\prod_\Omega$). However, test experiments showed explicitly that the C_5H + H channel is only open at collision energies larger than 86 kJ mol^{-1}; the C_5 + H_2 pathway was unobservable. Both alternative reaction channels in the tricarbon–acetylene reaction to give $C_4H_2(X^1\Sigma_g^+)$ + C(^3P_j) and $C_4H(X^2\Sigma^+)$ + CH($X^2\prod_\Omega$) are endoergic by 133 and 261 kJ mol^{-1} and hence closed, too. Therefore we can safely presume that although tricarbon molecules are in the primary beam, no reaction with the acetylene takes place under our experimental conditions.

Figs. 1 and 2 display the laboratory angular distribution and selected TOF spectra recorded at $m/e = 49$ (C_4H^+). The laboratory angular distribution is relatively narrow and extends over 30° in the scattering plane as defined by both beams. This suggests that the total available energy released into the translational degrees of freedom of the reaction products is relatively small. In addition, the laboratory distribution peaks close to the center-of-mass angle of $28.5 \pm 0.5°$, but is slightly forward scattered with respect to the dicarbon beam. Both figures do not depict solely the raw data, but also the computed curves. These are superimposed as solid lines and represent the best-
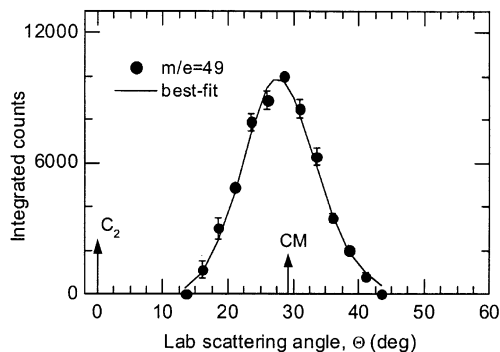
Fig. 1. Laboratory angular distribution of the C_4H product measured at $m/e = 49$ at a collision energy of 24.1 kJ mol^{-1}. Filled dots and error bars indicate the experimental data and the solid lines the calculated distribution with the best-fit center-of-mass functions.
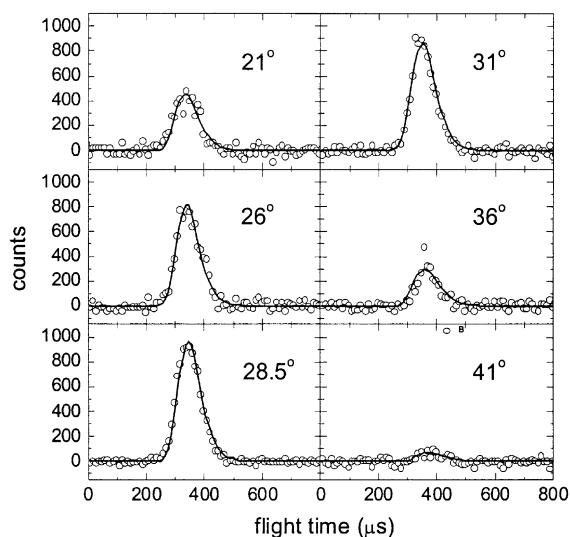
Fig. 2. Selected time-of-flight spectra ($m/e = 49$) at distinct laboratory angles for the C_4H reaction product at a collision energy of 24.1 kJ mol^{-1}. The open circles represent the experimental data, the solid lines the calculated fit.

fit achieved using the CM functions $T(\theta)$ and $P(E'_T)$ reported in Fig. 3.

The best fit CM angular distribution (Fig. 3, top) holds an intensity over the complete angular range and is forward scattered with respect to the primary beam; the intensity ratio at the poles was found to be $I(0°)/I(180°) = 2.0 \pm 0.2$. If we
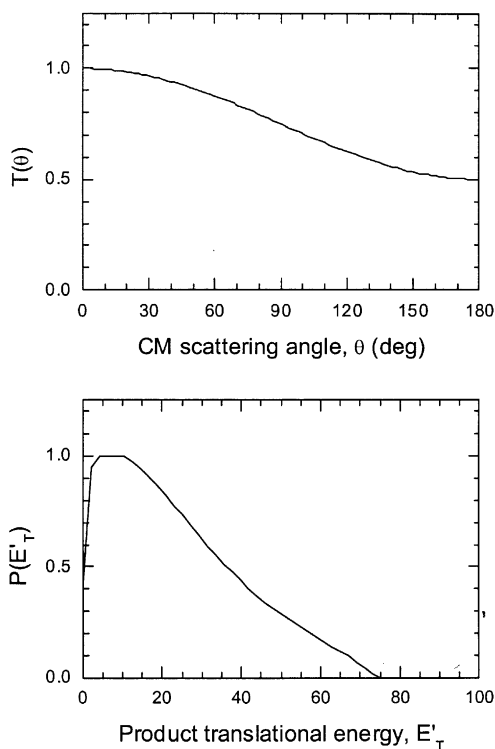
Fig. 3. Center-of-mass angular flux (top) and energy (bottom) distributions for the reaction of dicarbon with acetylene to form the butadiynyl isomer plus atomic hydrogen.

examine now the product translational energy distributions, we can see no clear peaking of the $P(E'_T)$, but rather a broad plateau from 4 to 12 kJ mol^{-1}. The fit is insensitive to the low energy range; hence the plateau can be extended to zero translational energy without changing the fit at all. This shape suggests that multiple reaction pathways in which C_4H_2 intermediates decompose without an exit barrier or with a moderate one. The best fit high energy cut-off of the distributions extend up to 75 kJ mol^{-1}; this energy limit can be cut by up to 10 kJ mol^{-1} without changing the fit significantly.

5. Discussion

In case of polyatomic systems it is always beneficial to combine the crossed beam data with electronic structure calculations on the potential

energy surfaces [20]. We would like to stress that potential energy surfaces alone cannot predict, for example, if the actual reaction is direct or indirect or the extent to which excited surfaces are involved. On the other hand, electronic structure calculations provide guidance for those systems in which experimental enthalpies of formation of products – often open shell species or labile molecules – are missing. Therefore, the present crossed beam experiment and the computations of the pertinent singlet and triplet C_4H_2 potential energy surfaces (Fig. 4) are highly complementary to expose the reaction dynamics of such complicated, multiatomic reactions.

First, we can inspect closer the CM translational energy distribution. The maximum translation energy ($E_{max} = 65$–75 kJ mol^{-1}) can be utilized to identify the nature of the products. Here, E_{max} is simply the sum of the reaction exoergicity plus the collision energy. Therefore, if we subtract the latter from E_{max}, the exoergicities of the reactions of ground state and excited state dicarbon molecules with acetylene reaction to form the C_4H isomer plus atomic hydrogen are calculated to be 45 ± 5 and 53 ± 5 kJ mol^{-1}, respectively. A comparison with the data from the NIST database to form the linear HCCCC isomer **p1** provides energies of 55 ± 8 and 63 ± 8 kJ mol^{-1}, respectively [21]. Therefore, the high energy cutoffs of the center-of-mass translation energy distribution suggest the formation of the butadiynyl radical, HCCCC. The formation of the cyclic C_4H isomers **p2** and **p3** can be safely excluded since the reaction endoergicities of 114.8 and 164.6 kJ mol^{-1} cannot be achieved considering a collision energy of 24.1 kJ mol^{-1}.

We try to address now the underlying reaction dynamics to form the butadiynyl radical on the singlet and triplet surfaces, respectively, and inspect the center-of-mass angular flux distribution $T(\theta)$ closer. This distribution shows intensity over the complete angular range suggesting that at least one reaction and/or one reaction micro channel follows indirect scattering dynamics. Keeping in mind that the reaction of $C_2(^1\Sigma_g^+)$ with acetylene was found to occur and to be fast, an inspection of the computed singlet surface (Fig. 4) comes to help in shedding light on the underlying mechanism.
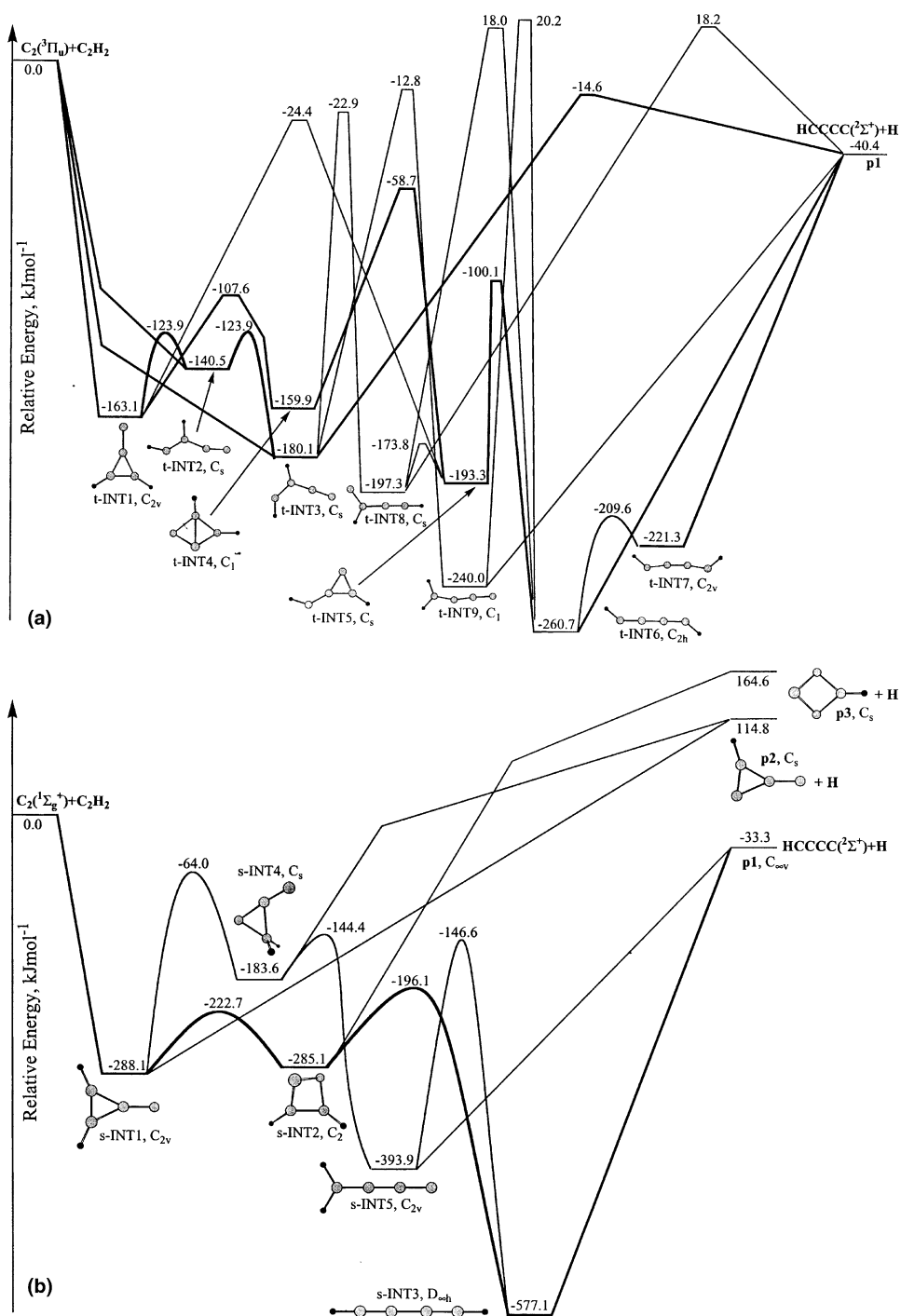
Fig. 4. Potential energy surface involved in the reactions of $C_2(X^1\Sigma_g^+)$ (bottom) and $C_2(a^3\Pi_u)$ (top) with acetylene. Point groups of the reactants, intermediates, and products are also included.

The butadiynyl isomer **p1** has been identified as the reaction product and, therefore, the decomposing singlet C_4H_2 intermediate must connect to **p1** + H. This condition is fulfilled only for **s-INT5** (butadienylidene) and **s-INT3** (diacetylene). The latter can be formed via addition of the singlet dicarbon molecule to the carbon–carbon triple bond of the acetylene molecule giving the cyclic intermediate **s-INT1** which rearranges via ring extension to **s-INT2**. This intermediate rearranges via ring opening to the diacetylene (**s-INT3**) species. An alternative pathway via **s-INT5** also follows through **s-INT1**, but then follows a hydrogen migration to form **s-INT4** and – after ring opening – **s-INT5**. Due to the barrier heights involved in the isomerization of **s-INT1** to **s-INT4** (+224.1 kJ mol^{-1}) and to **s-INT2** (+65.4 kJ mol^{-1}), we can conclude that the most favorable pathway involves formation of **s-INT1** from the separated reactants, followed by isomerization to **s-INT2**, ring opening to **s-INT3**, and emission of a hydrogen atom forming **p1**. What is the effect of intermediate **s-INT3** on the shape of the center-of-mass angular distribution? First, **s-INT3** is linear. This dictates that the diacetylene molecule as well as the linear butadiynyl product must be excited to B-like rotations. However, a 'symmetric' reaction intermediates such as the linear diacetylene molecule ejects a hydrogen atom with equal probability from the **HCCCCH** and **HCCCCH** positions into θ and $\theta - \pi$. Therefore, the formation of the butadiynyl radical via the decomposition of the diacetylene intermediate **s-INT3** on the singlet surface results necessarily in a forward–backward symmetric angular flux distribution from this microchannel.

However, the total center-of-mass angular distribution shows a pronounced forward scattering which cannot be explained solely by the contribution of the $C_2(X^1\Sigma_g^+) + C_2H_2(X^1\Sigma_g^+) \rightarrow$ HCCCC + H pathway (forward–backward symmetry). Therefore, at least one additional microchannel must exist; the latter must involve a 'non-symmetric' intermediate to account for a 'non-symmetrical', forward-scattered contribution to the CM angular distribution. This intermediate does not exist on the singlet surface. The only option would be the involvement of **s-INT5**; but our previous argumentation dismissed this contri-

bution of this structure to form the butadiynyl radical. Based on these considerations, the non-symmetric intermediate likely arises from the triplet C_4H_2 surface (Fig. 4). In the following sections, we discuss the potential involvement of several triplet intermediates successively. Due to the significant barriers of atomic hydrogen migration of 137 and 167 kJ mol^{-1} involved in the isomerization of **t-INT3** → **t-INT8** and **t-INT3** → **t-INT9** compared to the **t-INT2** → **t-INT3** process (16.6 kJ mol^{-1}), **t-INT8** and **t-INT9** likely do not play an important role in the underlying mechanism to form the butadiynyl radical. **t-INT6** and **t-INT7** cannot account for the forward scattering either. Further, since the reaction product **p1** has to rotate around the B axis, angular momentum conservation dictates that **t-INT6** and **t-INT7** have to be excited to B-like rotations. As a matter of fact, both structures are symmetric and may account solely for a forward–backward symmetric CM angular distribution, but not for a forward scattered ones. However, at the present point we have no possibility to verify or to dismiss the contribution of **t-INT6** and/or **t-INT7**. This leaves us with **t-INT1-5** as potential candidates for the forward scattered microchannel. **t-INT4** is only important in the isomerization to **INT6** and **INT7** via **INT 5**, but cannot decompose to HCCCC + H. Hence **t-INT4** and also **t-INT5** can be ruled out as the decomposing complexes. Therefore, only **t-INT1-3** remains. Even if **t-INT2** is formed, it cannot fragment to HCCCC plus atomic hydrogen but rearranges to **t-INT1** and/or **t-INT3**. Therefore, the fragmenting intermediate leading to the forward scattered contribution must be either **t-INT1** or **t-INT3**. **t-INT1** can be excluded as well: it cannot decompose to the butadiynyl radical but can isomerize solely to **t-INT4** and back to **INT2**; note, however, that **INT 4** was already dismissed. Henceforth, **t-INT3** is the only remaining intermediate. This structure fulfills all the necessary requirements to explain the experimentally found features. Firstly, the incorporated dicarbon unit and the leaving H atom are located on different sites of the rotation axis of **t-INT3**; this is crucial to account for the forward-scattered microchannel. Secondly, **t-INT3** can be formed via large impact parameter collisions; this is indicative for

dynamics of a reaction without entrance barrier as confirmed in our calculations. Finally, the short-lived **t-INT3** decomposes via an exit barrier; this is reflected also in this part of the CM translational energy distribution which peaks away from zero. On the other hand, the singlet diacetylene intermediate fragments without exit barrier, and therefore, can account for the part of the $P(E'_T)$ which peaks close to zero translational energy. In summary, both microchannels arising from **t-INT3** and **s-INT3** can well result in a broad translational energy distribution, which has been observed experimentally. We would like to stress that both microchannels form, indeed distinct butadiynyl products (Fig. 4). On the singlet surface, the attacking dicarbon unit as denoted in bold is incorporated between both carbon atoms which belonged to the acetylene molecule to form a HC**CC**C isomer. However, the dicarbon molecule adds to the acetylene molecule at the terminal carbon atom which results in an HCC**CC** isomer after hydrogen ejection. Although our investigations cannot unravel at the present stage the actual contribution of the initial collision complexes **t-INT1** vs **t-INT2** and **t-INT3**, the latter has been clearly identified as the fragmenting intermediate which accounts for the forward scattered microchannel; **t-INT1**, which can be formed by smaller impact parameter collisions, and **t-INT2** both rearrange finally to **t-INT3**. Also, the actual involvement of **t-INT6** and **t-INT7** remains subject to further studies.

Finally, we would like to address briefly alternative exit channels. Our experiments indicated the absence of the thermodynamically open $C_4(X^3\Sigma_g^-) + H_2(X^1\Sigma_g^+)$ pathway. This is supported by our electronic structure calculations since no exit transition state from any triplet C_4H_2 intermediate to $C_4(X^3\Sigma_g^-) + H_2 \ (X^1\Sigma_g^+)$ was located. The alternative exit channels to form c-$C_3H_2(X^1A_1) + C(^3P_j)$, c-$C_3H(X^2B_1) + CH(X^2\prod_\Omega)$, $CH_2(X^3B_1) + C_3(X^1\Sigma_g^+)$, or $C_2H(X^{2+}) + C_2H(X^2\Sigma^+)$ are all endoergic by 152, 246, 142, and 68 kJ mol^{-1}, respectively. Considering our collision energy of 24.1 kJ mol^{-1}, these channels are therefore closed at the collision energy utilized in the present experiment. Based on these considerations we can conclude that the butadiynyl radical and atomic

hydrogen are the sole products of the reactions of ground and excited state dicarbon molecules with acetylene in our experiment.

6. Conclusion

Our combined experimental and theoretical investigations on the reactions of ground state and electronically excited dicarbon molecules with acetylene suggest that only one channel, i.e., the formation of butadiynyl plus atomic hydrogen, is open in both cases. The reaction on the singlet surface has no entrance barrier, is indirect, and proceeds via addition of the dicarbon species to the carbon–carbon triple bond of the acetylene molecule. The cyclic C_4H_2 intermediate **s-INT1** rearranges to **s-INT2** which undergoes ring opening to form the diacetylene structure **INT3**. The latter decomposes without an exit barrier to the observed butadiynyl radical plus atomic hydrogen; angular momentum conservation dictates that the diacetylene intermediate as well as the radical product must be excited to B-like rotations. The fragmentation of this symmetric intermediate results in a forward–backward symmetric center-of-mass angular flux distribution. On the triplet surface, at least one additional microchannel leading to butadiynyl has been identified. The reaction starts also with an addition of dicarbon to the acetylenic bond, but this time only to the terminal carbon atom of the acetylene molecule to give **t-INT3**. This intermediate is short lived and fragments with an exit barrier of about 26 kJ mol^{-1} to the products. Hence the underlying dynamics of this microchannel account for the forward-scattered center-of-mass angular distribution. Note that **t-INT1** and **t-INT2** are also alternative entrance channels to the reaction; however both intermediates rearrange solely to **t-INT3**. Also, at the present stage we cannot quantify the contribution of the **t-INT6** and **t-INT7** structures.

Our studies allowed us also to extract for the first time the underlying reaction micro mechanisms of a dicarbon reaction with an alkyne on the molecular level and permit us now to include not only the rate constants of this important dicarbon

molecule reaction, but also the actual reaction products into pertinent kinetic models of combustion flames and of extraterrestrial environments. The butadiynyl radical has been observed widely in cold molecular clouds and also in circumstellar envelopes of carbon rich stars. Since the reaction of dicarbon has no barrier, the astronomically observed butadiynyl can be formed even in cold molecular clouds holding averaged translation temperatures of the reactants of 10 K. Finally, we did not only identify the reaction products, but proposed further the existence of the highly unstable cyclic intermediates. Since both dicarbon and acetylene are present in oxygen poor hydrocarbon flames, our results suggest that a laser based detection of these important reaction intermediates could be feasible.

Acknowledgements

References

[1] A.P. Baranovski, J.R. McDonalds, J. Phys. Chem. 66 (1977) 3300.
[2] W. Weltner, R.J. van Zee, Chem. Rev. 89 (1989) 1713.
[3] M.R. Combi, U. Fink, Astrophys. J. 484 (1997) 879.
[4] K.S.K. Swamy, Astrophys. J. 481 (1997) 1004.
[5] P. Rousselot, C. Laffont, G. Moreels, J. Clairemidi, A.A. 335 (1998) 765.
[6] S.B. Yorka, Astrophys. J. 88 (1983) 1816.
[7] A. Crawford, M.J. Barlow, MNRAS 311 (2000) 370.
[8] M. Martin, J. Photochem. Photobiol. A 66 (1992) 263, and references therein.
[9] N. Balucani, A.M. Mebel, Y.T. Lee, R.I. Kaiser, J. Phys. Chem. A 105 (2001) 9813.
[10] R.I. Kaiser, T.N. Lee, T.L. Nguyen, A.M. Mebel, N. Balucani, Y.T. Lee, F. Stahl, P.V.R. Schleyer, H.F. Schaefer III, Faraday Discuss. 119 (2001) 51.
[11] K.H. Becker, B. Donner, H. Geiger, F. Schmidt, P. Wiesen, Z. Phys. Chem. 214 (2000) 503.
[12] N. Balucani, O. Asvany, Y. Osamura, L.C.L. Huang, Y.T. Lee, R.I. Kaiser, Planet. Space Sci. 48 (2000) 447.
[13] R.I. Kaiser, N. Balucani, Acc. Chem. Res. 34 (2001) 699.
[14] R.I. Kaiser, J.W. Ting, L.C.L. Huang, N. Balucani, O. Asvany, Y.T. Lee, H. Chan, D. Stranges, D. Gee, Rev. Sci. Instr. 70 (1999) 4185.
[15] A.D. Becke, J. Chem. Phys. 98 (1993) 5648.
[16] C. Lee, W. Yang, R.G. Parr, Phys. Rev. B 37 (1988) 785.
[17] G.D. Purvis, R.J. Bartlett, J. Chem. Phys. 76 (1982) 1910.
[18] M.J. Frisch, GAUSSIAN 98, Revision A.7, Gaussian Inc., Pittsburgh, PA, 1998.
[19] MOLPRO is a package of ab initio programs written by H.J. Werner and P.J. Knowles with contributions from J. Almlóf et al.
[20] R.I. Kaiser, A.M. Mebel, Int. Rev. Phys. Chem. 21 (2002) 356.
[21] NIST database, Available from <http://webbook.nist.gov/>.